Study of methyl group rotations and primary relaxation in poly(vinyl methyl ether)

An experimental investigation using High Flux Backscattering Spectrometer at NCNR

Summer School on the Fundamentals of Neutron Scattering
NIST Center for Neutron Scattering
June 17-21, 2013

HFBS Team

Madhusudan Tyagi and Wei Zhou

Abstract

In this experiment, we will use elastic and quasi-elastic neutron scattering to examine the methyl group rotations and primary relaxation in poly(vinyl methyl ether). The goal of this hands-on measurement is to gain an understanding and appreciation of backscattering spectroscopy, get practical experience in obtaining the elastic and quasi-elastic data, reduce, analyze and interpret a set of these data.

I.   <u>Introduction</u>

Polymers are materials including plastics, rubbers, fibers, coatings and adhesives. The word polymer is derived from the Greek polys, which means 'many', and meros, which means 'part', in other words, a polymer is something that consists of many parts. A polymer in real life is a chemical substance composed of an enormous number of extremely large, usually chain-shaped molecules. These chain molecules (or chains) are in turn composed of 'many parts', in fact thousands of repeating units that form the links of the chains. A polymer is produced in a process called polymerization. In polymerization, small simple molecules called monomers (from the Greek mono, 'one' + meros, 'part') bond together to form the chain molecules of polymers. The repeating units (the links) of the polymer chains are chemically similar but not identical to the original monomer molecules. Polymers have a great technological significance because of their mechanical properties. They are utilized in the semi-crystalline form, as amorphous glasses and as rubbery elastomers. The diverse and, at times, unusual properties of polymers make them an object of high practical interest subject to continuously increasing research attention. If you look around, you will find that almost everything you see has some polymer in it!

II.   <u>Why Neutron Backscattering?</u>

The answer has to do with suitability of the length and time scales. As we all know, momentum transfer Q is inversely related with length scales under observation. So, we can consider Q as the power of our microscope we are using to probe the dynamical properties of a polymer. The Q values covered by HFBS (0.25Å^{-1} – 1.8Å^{-1}) correspond to length scales of 35Å to 4Å. This fits nicely with the length scale region of interest for small molecules and polymers. The length of a covalent bond is about 1.5Å which makes a "typical" monomer to be of the order of 5Å and larger.

Further more, by variation of the contrast between the structural units or molecular groups, complex systems may be selectively studied. In particular, the large contrast achieved by isotopic substitution of hydrogen by deuterium constitutes the most powerful tool for deciphering complex structures and dynamic processes in these materials. To give you an idea here are some of the incoherent (and coherent) scattering cross sections for common elements found in polymers: H: 80.5 (1.75) barns, D: 2.0 (5.5) barns, C: 0.0 (5.5) barns and O: 0.0 (4.2) barns. As the incoherent cross section of hydrogen is much larger, the total scattering observed in a quasi-elastic neutron scattering (QENS) experiment will be dominated heavily by incoherent scattering from hydrogen in the sample. This allows us to selectively study the motions we are interested in or separate more complex systems into smaller pieces. For example, if we want to study methyl group rotations in poly(vinyl methyl ether) (PVME), partially deuterated samples of PVME can be studied where only methyl group is protonated.

III.   <u>What we will do in this experiment?</u>

We will study methyl group rotations and primary relaxation, or so called α-relaxation, in poly(vinyl methyl ether) (PVME). The monomeric/chain view of PVME is shown below:

[-CH$_2$-CH-]$_n$
|
O-CH$_3$

H$_2$C=CH—O—CH$_3$
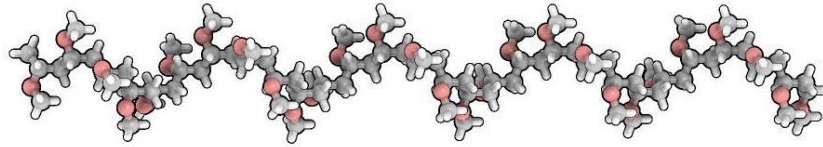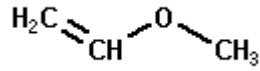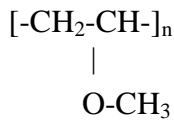
This simple polymer with a simple chain structure can show very different kinds of motions depending on its thermal state. To give you a qualitative picture, below is a general sketch of polymer dynamics as a function of temperature.
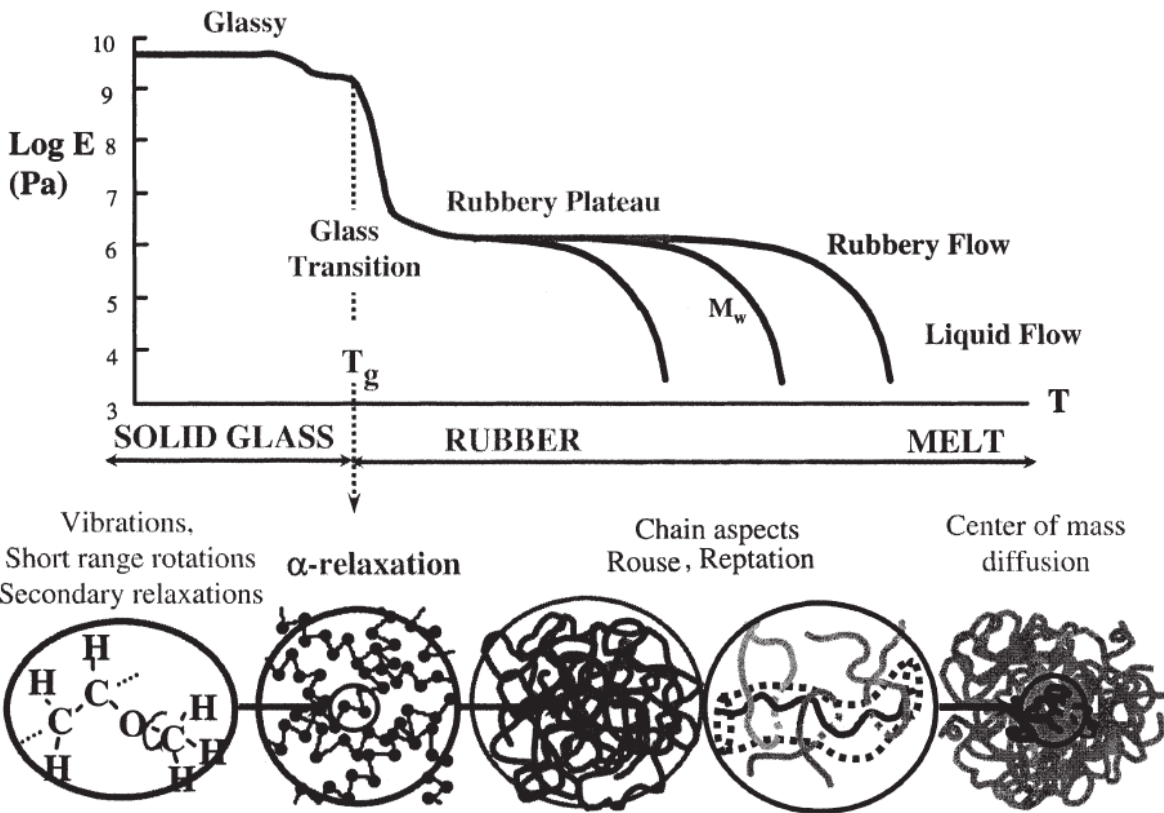

Fig.1: *Richness of dynamic modulus in a bulk polymer and its molecular origin. The associated length scales vary from the typical bond length (≈Å) at low temperatures to interchain distances (≈10Å) around the glass transition. In the plateau regime of the modulus typical scales involve distances between "entanglements" of the order of 50–100Å. In the flow regime the relevant length scale is determined by the proper chain dimensions.*

At low temperature the material is in the glassy state and only small amplitude motions like vibrations, short range rotations or secondary relaxations are possible. For example, the secondary β-relaxation and the methyl group rotations can be observed below the glass transition, T_g. At high frequencies the vibrational dynamics, in particular Boson peak, characterize the dynamics of polymers. The secondary relaxations cause the first small step in the dynamic modulus of such a polymer system.

Q: Can we observe secondary relaxations in a backscattering experiment? Hint: See relaxation map (Fig.4)!

At the glass transition temperature T_g the primary relaxation (α-relaxation) becomes active allowing the system to flow. The length scale associated with α-relaxation is the typical inter-chain distance between two polymer chains. In the dynamic modulus, the α-relaxation causes a significant step of typically three orders of magnitude in strength.

The following rubbery plateau in the modulus relates to large scale motions within a polymer chain. Two aspects stand out. The first is the entropy-driven relaxation of fluctuations (out of equilibrium). Secondly, these relaxations are limited by confinement effects caused by the mutually interpenetrating chains. The confinement effects can be described in terms of a tube following the coarse grained chain profile. Motion is only allowed along the tube profile leading to the reptation process – the snake-like motion of a polymer chain.

Q: Can we observe reptation and center of mass diffusion in polymers by neutron backscattering in this experiment?

Now, after having a qualitative picture of polymer dynamics, let us go back to our experiment. For a successful experiment, one has to pick a suitable pressure/temperature environment to match the time scales of the process under investigation (α-relaxation or methyl group rotations) with the instrument we are working on. This can be done if one has some prior knowledge of sample dynamics by other experimental techniques e.g. dielectric, NMR or spectroscopy. However, care has to be taken as neutron scattering has Q (equivalently length scale) dependent time scales and therefore, it becomes important on what Q values the time scales will match with other techniques. This obviously depends on the system under investigation.

We have a better solution to resolve this issue! We can use what is called 'elastic mode' and run a fixed energy window scan with temperature or pressure to see when the time scales of α-relaxation (or methyl group rotation) enter into backscattering time window as a function of Q. Therefore, in this experiment, we will start with a fixed window scan (FWS), covering the entire temperature range of interest from 4K to 400K. The pressure will be held constant at ambient but can be varied in other experiments. Based on the FWS, we will pick up suitable temperatures for α-process and run the dynamics.

<u>Sample and Sample Environment Details</u>:

PVME is commercially available as a 50% mixture with water. Water can be evaporated and a suitable film of required thickness can easily be obtained. The film is then rolled into an annulus (cylinder) and inserted into the sample can. The annular geometry was selected to minimize the amount of corrections necessary in the data reduction. If the sample is too thick, then a significant number of the neutrons may get absorbed. This *self-shielding* depends on the absorption cross-section of the sample as well as the geometry. For an annular geometry where the neutron sees only a thin portion of the sample, the corrections are negligible. Another concern when determining sample design is minimization of *multiple scattering*. In an ideal neutron scattering measurement, we would like for the neutron to scatter once within the sample before reaching the detector. In practice, the neutrons can undergo several scattering events within the sample and/or be absorbed by the sample. The number of events increases with the thickness of the sample illuminated by the beam. One often used rule-of-thumb is to design sample geometry where 90% of the incident neutrons are transmitted in the forward direction. This is a good compromise between signal and the effects of multiple scattering. Such a sample is usually referred to as a *10% scatterer*. Using the known scattering and absorption cross-sections for PVME and the geometry, one can calculate the desired thickness. For PVME in an annular cell the approximate thickness for 90% transmission in the forward direction is around *0.20 mm*. The sample film we have made is about **0.25mm** in thickness.

Q: How many times does the beam go through the sample before reaching the detectors?

The answer to the question posed above can have important consequences for your experiment. If the beam passes through the sample twice (for instance) and the sample has an appreciable neutron absorption cross-section, then the intensity at the detectors will be lower than if the beam had only passed once through the sample. Additionally, a beam which passes twice through a strongly scattering sample can produce an energy-dependent background. For more details on these points, see Appendix A.

The sample can will be placed in a top loading closed-cycle refrigerator capable of reaching a base temperature of 4 K. The measurements performed here will cover a temperature range of 4K -400K. We will use a combination of low-T and high-T sample sticks to cover the entire temperature range.

IV.   Modes of Spectrometer and Data Reduction Details

We can use HFBS spectrometer in two different modes to extract the dynamical features of the sample under investigation.

A.   Fixed Window Scans:

For reactor based neutron backscattering spectrometers, "Fixed window scans" or "elastic scans" are very powerful for getting a fast overview of the dynamics of a system and are often the starting point for quasi-elastic measurements. In this mode, we choose to count the neutrons with fixed initial and final wave vectors which results in analyzing neutrons scattered within a fixed energy window. To do so, we stop the moving monochromator (see below) and then change the external parameters like temperature and pressure and record the intensity. We can even assign a time scale to fixed window scans based on the instrumental resolution. In our case, assuming a FWHM of about 0.8μeV, the slower limit would correspond to about 10ns. Dynamic processes on a time scale slower than the instrumental resolution are not resolved and thus are counted within the "elastic window". Faster motions of scattering particles can be resolved and will induce an energy loss or gain of the scattered neutrons, which then are no longer reflected by the analyzers to the detectors. One observes a decrease of the elastic window intensity as function of increasing temperature. Therefore, elastic or fixed window scans give a quick overview of the onset of motions faster than the time scale corresponding to the energy resolution (~10 ns) and therefore, can be used to choose suitable temperatures for dynamic measurements.

B.   Quasi-elastic Neutron Scattering:

The HFBS spectrometer is configured in an *inverse scattering geometry*. This means that the energy of the neutron incident on the sample is varied while the final energy of the neutrons reaching the detectors is fixed.
A summary of the basic principle of operation of HFBS is outlined below (for more details on the instrument including a schematic see Appendix B)

1. The "white" beam of neutrons produced by the reactor is velocity selected to yield neutrons that have energies around the desired energy of 2.08 meV. These neutrons are further focused in energy by a rotating phase space transform chopper and scattered towards the Doppler monochromator. The energy focused neutrons are backscattered from the Doppler monochromator thus selecting incident neutron energies, E_i, dependent upon the speed of the monochromator when reflected. While the Doppler is at rest, only neutrons with energies of 2.08 meV are backscattered from the monochromator. This is due to the lattice spacing of the Si hexagons that tile the surface of the monochromator.

2.   The reflected neutrons from monochromator interact with the sample and are scattered from the sample with a distribution of energies.

3.   Only neutrons with a particular scattered energy, E_f, reflect from the analyzer array into the detectors. Identical Si hexagons comprise the analyzer system, thus the backscattered neutrons all have energies of 2.08 meV. The energy transfer imparted on the sample is defined as $E=E_i-E_f$.

4.   Neutrons scattered from the sample in a particular direction backscatter from particular analyzers and are counted one of the 16 detectors. This direction corresponds to the scattering angle, 2θ.

Q: What is the energy range of the neutrons incident on the sample, E_i?

Note: this next section will be conveyed using energy, wavelength and velocity. These values are generally constant for HFBS; the neutrons that reach the detectors have energies of 2.08 meV, wavelengths of 6.27 Å and velocities of 630.8 m/s.

Given the scattering angle, 2θ, and energy transfer, E, we may calculate the magnitude of the momentum transfer delivered to the sample, Q. Kinematical arguments lead to the following relationship between 2θ, E, E_i, and Q:

$$\frac{\hbar^2 Q^2}{2m_n} = 2E_i - E - 2\sqrt{E_i(E_i - E)}\cos(2\theta) \qquad \text{(eq.1)}$$

where m_n is the mass of the neutron and $\hbar$ is Planck's constant.

The data acquisition system records the number of detector counts as a function of initial neutron velocity, v_i, where v_i is related to the instantaneous monochromator velocity, v_m, and the Bragg velocity of the neutrons with velocity 630 m/s, v_B, via $v_i = v_B + v_m$. The energy transfer to the sample, due to a Doppler shift of the neutron energies, is given by,

$$E = 2E_B\left(\frac{v_m}{v_B}\right) + E_B\left(\frac{v_m}{v_B}\right)^2 \qquad \text{(eq.2)}$$

where E_B is the Bragg energy of neutrons with wavelength 6.27 Å, is calculated and written to the raw data file. This calculation is done using an encoded Doppler drive that provides information as to the acceleration as a function of position. The energy change is derived from this acceleration. Note that the motion of the monochromator is time-dependent, allowing the variation of E_i necessary to an inverse geometry spectrometer.

Q: Can you think of a way to change the incident neutron energies without moving monochromator?

The raw data measured is recorded as $N(2\theta_j, E_k) = N_{jk}$, the number of neutrons detected in detector j (at scattering angle corresponding to $2\theta_j$) with an energy transfer to sample of E_k. The quantity which reflects the dynamics of the scattering system most directly is $S(Q, E = \hbar\omega)$, the dynamic structure factor. What we measure, N_{jk}, is closely related to the partial differential cross-section, $d^2\sigma/d\Omega dE$. This can be written in terms of the various instrument-dependent parameters and the number of counts received in the detectors,

$$\left[\frac{d^2\sigma}{d\Omega dE}\right]_{j,k} = \frac{N_{j,k}}{\eta(E_f)} \frac{A\eta(FC)}{N(FC)} \gamma_j \frac{1}{\rho_N V} \frac{1}{\Delta\Omega_j} \frac{1}{\Delta E} \qquad \text{(eq.3)}$$

where,

$\left(\dfrac{A\eta(FC)}{N(FC)}\right)$: *the monitor normalization* of incident beam area (A) times the beam monitor efficiency ($\eta(FC)$) divided by the number of counts received by the beam monitor. (FC) indicates the type of detector, a fission chamber.

$\dfrac{\gamma_j}{\eta(E_f)}$: *the vanadium normalization* of the detector intensity with the intensity scaling factor γ_j divided by the efficiency of the detector.

ρ_N: number density of scatterers in the sample
V: volume of sample illuminated by the beam
ΔE: energy channel width or binning of the dynamic range
$\Delta\Omega j$: solid angle subtended by detector or analyzer angular coverage

We can obtain the dynamic structure function, S(Q,E), using the first Born approximation (i.e. a single scattering event dominates the response of the scattering system) via

$$S(Q,E) = \frac{4\pi}{\sigma} \frac{k_i}{k_f} \frac{d^2\sigma}{d\Omega dE} \qquad \text{(eq.4)}$$

where,
σ: scattering cross-section
k_i: incident neutron wave vector
k_f: final neutron wave vector
Note that for a sample in thermal equilibrium, the *detailed balance condition* is satisfied,

$$S(Q,-E) = e^{-\frac{E}{kT}} S(Q,E) \qquad \text{(eq.5)}$$

where E is the sample energy gain. This condition is a technical way of saying that it is more likely that a sample will give energy to the neutron when the sample is at a high temperature as compared to when the sample is at a low temperature.

V.   Tools to study Polymer Dynamics:

The neutron intensity after correction gives the experimental scattering function $S_{exp}(Q, \omega)$ as a function of energy transfer (E=ℏω). The theoretical scattering function S(Q, ω)

which gives the dynamics of the polymer in quasielastic neutron scattering experiment is given by [1]

$$S_{theo}(Q,\omega) = DWF\{f(Q)\delta(\omega) + [1- f(Q)]S_{QE}(Q,\omega)\} + S_{IN}(Q,\omega) \qquad (eq.6)$$

where DWF is the Debye-Waller Factor that describes the attenuation of neutron scattering as a result of temperature variation, $f(Q)$ represents the elastic incoherent scattering factor that has zero value for diffusive motion. $\delta(\omega)$ is Delta function corresponding to zero frequency. $S_{QE}(Q,\omega)$ and $S_{IN}(Q,\omega)$ are the quasi-elastic and inelastic incoherent scattering functions respectively. $S_{IN}(Q,\omega)$ can also be used to describe the processes that are much faster than one's instrument frequency window in the form of a flat background. In case of α-relaxation, $f(Q)$ becomes zero and the above eq. takes a simple form:

$$S_{theo}(Q,\omega)=DWF\times S_{QE}(Q,\omega)+S_{IN}(Q,\omega) \qquad (eq.7)$$

It is important to remember that the general eq.6 (or eq.7) has to be convoluted with experimental resolution function before it can be fitted to experimental measured scattering function. The resolution function is the slowest possible scattering function that can be measured at a given instrument. For more details on resolution function, please see appendix C. **As for scattering function, hereafter, we will talk only about theoretical scattering function.**

Q: Can we measure resolution function using our own sample for this experiment?

As noted above, hydrogenated sample of PVME will scatter incoherently and almost all the intensity will be incoherent in nature. The incoherent intensity reveals the incoherent scattering function, $S_{inc}(Q,\omega)$, that is related via Fourier transformations to the intermediate incoherent scattering function, $S_{inc}(Q,t)$, and with the self-part of the Van Hove correlation function, $G_{self}(r,t)$. In the classical limit, $G_{self}(r,t)$ is the probability of a given nucleus being at distance r from the position where it was located at a time t before. Thus, incoherent scattering looks at correlations between the positions of the same nucleus at different times. Therefore, in backscattering measurements, we observe a given particle's self correlation function $S(Q,t)$ in frequency domain and with its time (frequency) evolution, we can track how the molecule is diffusing in space (through Q dependence) and time.

Modeling of Intermediate or Dynamic Scattering function:

For the sake of clarity and in order to follow general polymer literature, we will discuss models in time domain i.e. for scattering function $S(Q,t)$. Intermediate scattering function $S(Q,t)$ is related with dynamic scattering function $S(Q,\omega)$ by Fourier transform (FT).

In case of simple or continuous diffusion, the scattering function is found to be simple exponential in the form [1]:

$$S(Q,t) = A(Q,t)\exp(-DQ^2t) \tag{eq.8}$$

In the above eq., A(Q,t) is well known Debye Waller Factor and D is the translational diffusion constant. In this case, relaxation is characterized solely by its initial slope DQ^2. However, if the simple diffusion does not occur, then the scattering function usually shows departure from simple exponential shape. In literature, this departure from simple exponential form is quite often termed as stretched exponential. In this case, the decay of *S(Q,t)* can be well described by the so-called *Kohlrausch-Williams-Watts (KWW) function* [2]:

$$S(Q,t) = A(Q,t)\exp\left[-\left(\frac{t}{\tau_\alpha(Q,T)}\right)^{\beta(Q,T)}\right] \tag{eq.9}$$

$\tau_\alpha(T)$ is the associated characteristic relaxation time and β is the stretching parameter ($0 < \beta < 1$). The stretching parameter β, in general, is a function of temperature and Q. However, it is found that for small molecules these dependences are very strong while polymer systems show less or no Q and temperature dependence.

The pre-factor *A(Q,T)* in eq.9 is a generalized Lamb-Mossbauer factor (LMF) or Effective Debye-Waller factor (DWF) accounting for processes occurring on time scales faster than time scales we are investigating. As we all know, in case of crystal samples, the mean vibration around the equilibrium position is found to be Gaussian. Following the same analogy, we can define effective DWF as:

$$A(Q,t) = \exp\left(\frac{-Q^2 <u^2>}{3}\right) \tag{eq.10}$$

It is characterized by an effective mean squared displacement of the proton $<u^2>$ which is found to be temperature dependent.

Q: How does the effective DWF in polymers differ from actual DWF in crystals?

A relationship between Simple exponential and KWW functions:

Although, simple exponential and stretched exponential functions seem identical, it is not possible to formulate an expression to have a relationship between them. The stretched exponential can be written as:

$$\exp\left[-\left(\frac{t}{\tau}\right)^{\beta}\right] \approx \sum A_i \exp\left(-\frac{t}{\tau_i}\right)$$ (eq.11)

which is a collection of individual exponentials, indicating, that a stretched exponential comprises of many simple exponential with a distribution of relaxation times. This distribution function can be visualized better if we convert everything to frequency domain. The simple exponential function of eq.8 can be converted to frequency domain by Fourier Transform and it turns into a well defined Lorentzian function:

$$S(Q,\omega) = A(Q,\omega)\frac{\Gamma(Q)}{\hbar^2\omega^2 + \Gamma^2(Q)}$$ (eq.12)

Similarly, a stretched exponential function can also be converted into frequency domain using a weighted distribution of Lorentzians at different frequencies [3]. Fig.2 shows such distribution functions that will generate corresponding stretched exponential function for different β values (shown in figure). Notice, how the distribution function stretches towards higher frequencies as β decreases!
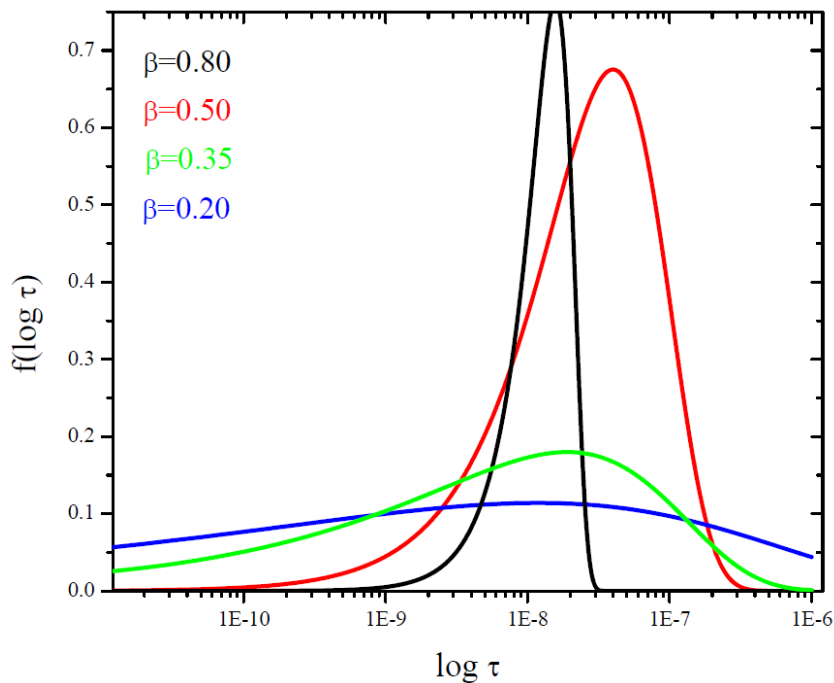

Fig.2: Sketch of distribution functions for different β values.

Q: Why is KWW a better approach than a simple exponential or Lorentzian for polymers?

Fitting of Experimental Data:

We will fit QENS data for PVME at different temperatures to FT of KWW function using DAVE [4] software. In the DAVE program, we have a choice a choice of model functions to fit the data according to our needs. FT of KWW model is listed as "ft_KWW" in the available functions. As we measure Fourier transform of intermediate scattering function, therefore, it is essential either to FT the data into time domain or FT the KWW function in time domain and then fit that to the frequency data. As we have limited energy window at backscattering, the Fourier transformed data in time domain will be limited by errors caused by truncation limits and so on. Therefore, it is better to FT the model function into frequency domain and fit that to the measured $S(Q,\omega)$.

In the DAVE program, if the ft_KWW function is chosen then FT of model function is performed, convoluted with experimental resolution and then it is fitted to experimental data in frequency domain.

The non-Arrhenius temperature-dependence of the relaxation time:

The temperature dependence of relaxation time or diffusion constant provides an excellent view of what might be the mechanism of diffusion or relaxation of the molecules in your sample on microscopic scale. It is well known that for simple diffusive process (or thermally activated processes), the temperature dependence is usually Arrhenius. However, if molecular mechanism of the process under investigation is not thermal activation, then a different temperature dependence is observed. For glass forming liquids and polymers, the relaxation time shows a dramatic increase when the glass transition temperature region is approached and, therefore, cannot be parameterized with Arrhenius-like temperature dependence. This temperature dependence is usually well described in terms of the so called Vogel-Fulcher temperature dependence [5]:

$$\tau_\alpha(T) = \tau_{\alpha 0} \exp\left[\frac{B}{T - T_0}\right] \qquad \text{(eq.13)}$$

where $\tau_{\alpha 0}$ is the relaxation time at infinite temperature, B is an activation energy constant and T_0 is the Vogel-Fulcher temperature. This temperature dependence is expected if one assumes a model where molecular cooperation is required for relaxation rather then individual thermal equilibration after a temperature change. This temperature dependence also predicts rapid increase in the relaxation time as one cools the sample towards glass transition temperature.

Q: What effect will cooperativity of molecules have on the relaxation time as you cool down?

Arrhenius-T dependence below T_g:

Below T_g, in the glassy state the main dynamic process is the β-process and methyl group rotations. In crystalline materials, methyl group rotations exhibit inelastic peaks in spectra e.g. in case of methyl iodide peaks show up at $\pm$ 2.4μeV [6]. In contrast to α-relaxation, methyl group rotations do not require any cooperation from the neighboring molecules and therefore, can be categorized as thermally activated process. However, in case of polymers, the gradual change in potential due to the disorder of amorphous systems, these peaks change position continuously and eventually, give rise to a weak quasi-elastic signal around the elastic peak. Such methyl group rotations can be explained in terms of so-called "rotational rate distribution model" which assumes a distribution of tunneling lines that follows from distribution of potential barriers for different methyl groups in polymer sample [7].

Q: Is there any way to verify (at least qualitatively) that individual tunneling lines turn into quasi-elastic signal in disordered systems? Hint: Think of toluene!

The temperature dependence of average FWHM as a function of temperature is found to be Arrhenius, and, therefore, support the thermally activated picture for methyl group rotations.
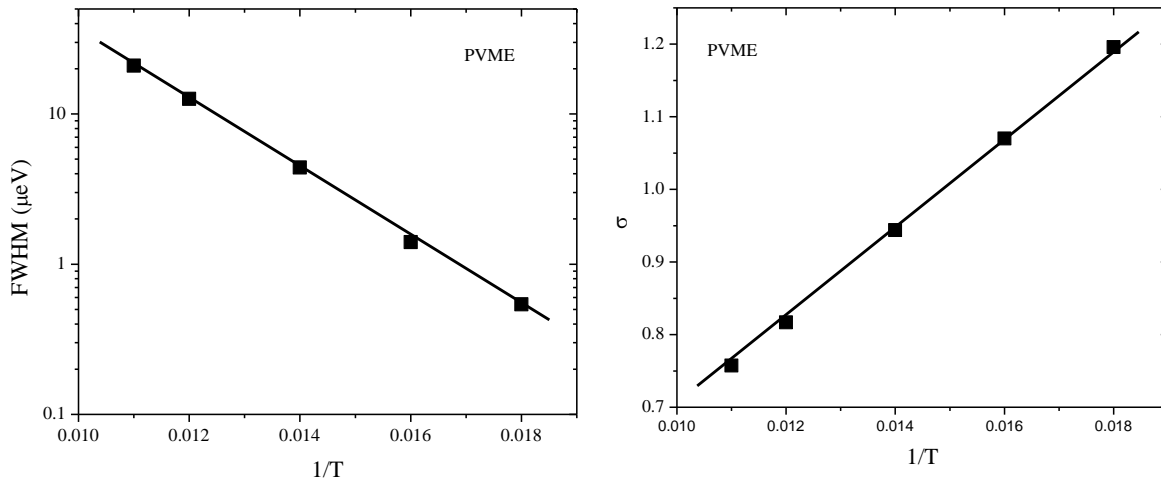

Fig.3: FWHM and width of distribution function as a function of temperature for methyl group rotation in Poly(vinyl methyl ether). FWHM and σ correspond to full width at half maximum of Lorentzian and the width of distribution function, respectively. Note increasing width of distribution as temperature decreases.

Below is a complete relaxation plot in polymers above and below T_g for polyisoprene. Notice, the Arrhenius temperature dependence of methyl group rotation while α-relaxation follows VFT eq. (eq.13)
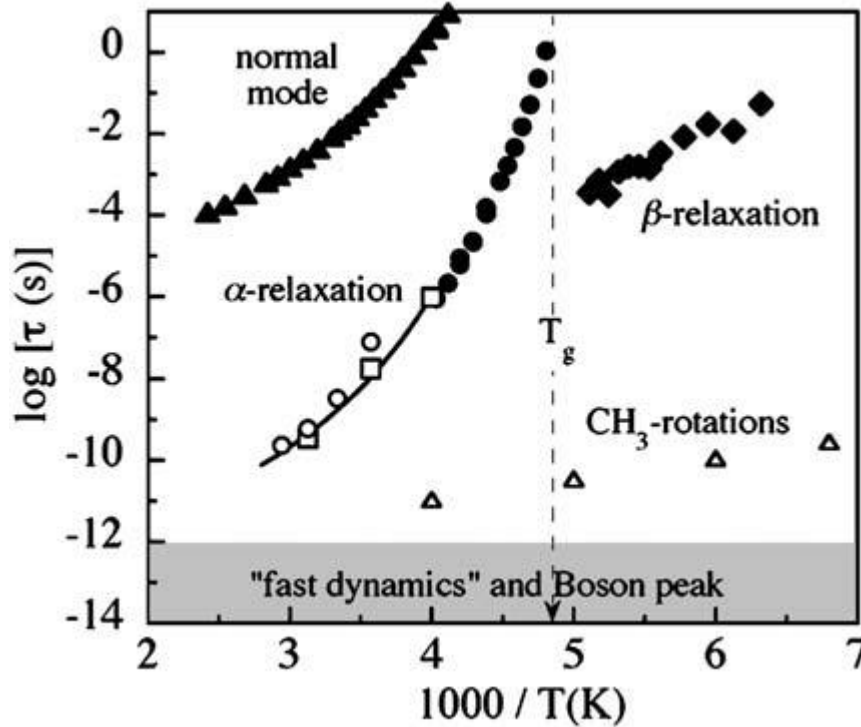

Fig.4: A complete relaxation map for one of the famous polymers, polyisoprene by different experimental techniques [8]. α-relaxation at low temperatures is covered by dielectric spectroscopy. Open symbols belong to neutron scattering measurements.

Q dependence of relaxation times:

Extensive studies of polymers by BS, DCS and NSE in the past has shown a way to model the Q dependence of relaxation times. It was found that the Q-dependence of τ_α can approximately be described by a power law determined by the stretching exponent β [9]:

$$\tau_\alpha(Q,T) = a_0(T)Q^{-2/\beta} \qquad \text{(eq.14)}$$

where $a_0(T)$ does not depend on Q. As polymers show typical values for β less than unity, above eq. predicts stronger Q-dependence than that characteristic of simple diffusion (Q^{-2}).

Q: Did you find $Q^{-2/\beta}$ law in PVME?

Now, let us combine what we have learned so far in eq.9 (from eq.10 and eq.14):

$$S(Q,t) = \exp\left(-\frac{<u^2>Q^2}{3}\right) \times \exp\left[-\left(\frac{t}{a_0 Q^{-2/\beta}}\right)^\beta\right]$$ (eq.15)

If we simplify above eq., it looks like this:

$$S(Q,t) = \exp\left(-\frac{\left\{2<u^2>+6\left[\dfrac{t}{a_0(t)}\right]^\beta\right\}}{6}Q^2\right)$$ (eq.16)

Now, let us see if we can learn something about the nature of dynamics of PVME chains from the above eq. It is well known that for simple liquids where simple diffusion takes place, calculated mean squared displacement varies as $<r^2(t)> \sim t$. In this case, intermediate scattering function is Gaussian and is given by:

$$S^{Gauss}(Q,t) = \exp\left[-\frac{<r^2(t)>}{6}Q^2\right]$$ (eq.17)

If we compare eq.16 with the above eq., it is clear that PVME chains follow Gaussian behavior as long as the power law for relaxation time (eq.14) is observed and mean squared displacement varies as:

(eq.18)

$$<r^2(t)> = 2<u^2> + 6\left[\frac{t}{a_0(T)}\right]^\beta$$

Let's have a look at the MD simulation results on PVME. As you can see, indeed, MSD increases as $\sim t^\beta$ in the intermediate time scales where the dynamics by backscattering is observed.
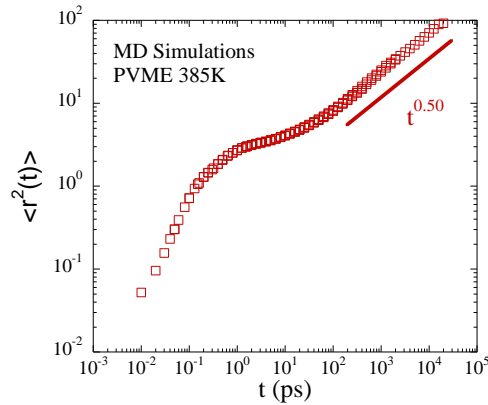
Fig.5: Mean squared displacement calculated by MD simulations for hydrogens of PVME at 385K. At very short time scales, so-called ballistic regime is observed which is followed by release of caging as plateau. α-relaxation can be seen in ns time scale.

This proves the Gaussian character of Van Hove correlation function for PVME chains at these time scales. This is somewhat similar to simple diffusion in case of small molecules but modified due to the chain connectivity and amorphous nature of PVME through the shape parameter β.

Q: Would you expect Gaussian character to appear at higher or lower Q values and why?

Time temperature superposition:

The time–temperature superposition, implying that the functional form does not appreciably depend on temperature. For instance, mechanical or rheological data corresponding to different temperatures can usually be superimposed if their time/frequency scales are shifted properly taking a given temperature T_R as reference. Time- temperature superposition is a procedure that has become more important in the field of polymers to observe the dependence upon temperature on the change of viscosity of a polymer which is indirectly related with relaxation time. Time-temperature superposition avoids the inefficiency of measuring a polymers behavior over long periods of time at a specified temperature by utilizing the fact that at higher temperatures and shorter time the polymer will behave the same.

Q: Do you expect time temperature superposition to hold in the case of PVME?

VI.   **References:**

1]   M. Bee, *Quasi-elastic Neutron Scattering*, Adam Hilgor, Bristol (1988).

2]   G. Williams and D. C. Watts, *Trans. Faraday Soc.* **66**, 80 (1970).

3] The KWW function can be generated in frequency domain using the weighted superposition of Lorentzian functions as:

$$\Phi_{KWW}(\omega) = \int f(\log\tau)\frac{\omega\tau}{1+\omega^2\tau^2}d(\log\tau)$$

where the distribution function f(log τ) is given by

$$f(\log\tau) = \ln\left(\frac{b}{2\pi(1-b)}\right)^{1/2}\left(\frac{\tau}{\tau_R}b\right)^{b/(2(1-b))}\exp\left[-(1-b)\times\left(\frac{\tau}{\tau_R}b\right)^{b/(1-b)}\right]$$

In the above eq., the parameters b and τ_R are related with β and τ in KWW eq.9 (See ref: D. Gomez and A. Alegria, J. Non Cryst. Solids. **287**, 246 (2001)).

4] More information about DAVE can be found at

http://www.ncnr.nist.gov/dave

5] H Vogel, Phys. Z **22**, 645 (1921); G. S. Fulcher, J. Am. Chem. Soc **8**, Pages 339 and 789

6] M. Prager, J. Stanislawski, W. Hausler, J. Chem. Phys. **86**, 2563 (1987).

7] Rotational Rate Distribution Model (RRDM) is an extension of methyl group modeling in crystals to disordered polymer systems. Due to the existence of the structural disorder, which is inherent to the glassy state, the methyl groups in a glassy polymer have different local environments arising from both the lack of regularity of the main-chain conformation and the different local packing conditions. This manifests itself in different rates of rotation. Therefore, incoherent scattering function is generalized by assuming a continuous distribution of jumping rates g(logτ):

$$S(Q,\omega) = f(Q)\delta(\omega) + \{1-A(Q)\}\int_{-\infty}^{\infty}g(\log\Gamma)\frac{1}{\pi}\frac{\Gamma}{\Gamma^2+\omega^2}d(\log\Gamma)$$

where g(logΓ) is assumed to be Gaussian-like in shape:

$$g(\log\Gamma) = \frac{1}{\sigma\sqrt{2\pi}}\exp\left[-\frac{1}{2\sigma^2}\log^2\left(\frac{\Gamma}{\Gamma_0}\right)\right]$$

8]   D. Richter, M. Monkenbusch, A. Arbe and J. Colmenero, *Neutron Spin Echo*, Adv. Polymer Sci. **174**

9]   J. Colmenero, A. Alegria, A. Arbe and B. Frick, Phys. Rev. Lett., 69 478 (1992)

Appendix A

Effects of the Sample Geometry on Self Shielding and Multiple Scattering

One must consider a number of issues when determining appropriate sample geometry. A naïve philosophy in designing sample geometry is to make the sample as big as possible in order to obtain as many scattering events in the shortest possible time. Unfortunately optimization of the experiment is not as simple as this. Sample design involves a careful consideration of the composition of the sample in terms of its scattering and absorption cross-sections.

In an inverse geometry spectrometer like HFBS where the beam passes through the sample twice one must consider *self-shielding* effects which reduce the intensity received at the detectors via absorption. In general absorption in the sample is proportional to the neutron wavelength. On a backscattering spectrometer using Si(111), E_i= 2.08 meV, λ= 6.27 Å, which results in the cross section for absorption being 3.5 times larger than for thermal neutrons with 1.8 Å.

In order to understand the extent to which you have to correct for multiple scattering/self-shielding it is important to know how strong a scatterer/absorber your sample is. The transmission in the forward direction ($2\theta = 0$) is often calculated and expressed in terms of a percentage of the incident beam that is scattered/absorbed. For instance, a flat plate sample with total scattering cross-section, $\sigma_{tot} = \sigma_{inc} + \sigma_{coh}$, and absorption cross-section, σ_{abs}, will have a scattering and absorption determined by

$$scattering = 1 - \exp\left(-\frac{\mu_s d}{\sin(\pi - 2\theta)}\right) \qquad \text{(flat plate)} \qquad \text{A1}$$

$$absorption = 1 - \exp\left(-\frac{\mu_{abs} d}{\sin(\pi - 2\theta)}\right) \qquad \text{(flat plate)} \qquad \text{A2}$$

where 2θ is the angle of orientation of the slab with respect to the incident beam direction, d is the thickness of the slab sample, and μ is the scattering coefficient (inverse scattering length in cm^{-1}) determined by

$$\mu_S = N_A \sigma_{tot} \rho / M \qquad \text{A3}$$

$$\mu_{abs} = N_A \sigma_{abs} \rho / M \qquad \text{A4}$$

where N_A is Avogadro's number (6.022×10^{23} mole^{-1}), ρ is the mass density of the sample material (in g/cc), and M is the molecular weight of the sample in g/mol. On the other hand an annular sample cell has a scattering/absorption in the forward direction determined by

$$scattering = 1 - \exp(-\pi \mu_s d) \qquad \text{(annular cell)} \qquad \text{A5}$$

$$absorption = 1 - \exp\left(-\pi\mu_{abs}d\right) \qquad\qquad \text{(annular cell)} \qquad\qquad \text{A6}$$

where the inverse scattering absorption lengths are calculated as described above (eqs. A3 and A4) and d is the wall thickness of the annular sample. Equations (A5) and (A6) are good approximations for the cases where $\exp(-\pi\mu d) > 80\%$.

We illustrate the self-shielding corrections for a vanadium sample ($\sigma_s(1.8\text{ Å}) = 5.10$ barn and $\sigma_{abs}(1.8\text{ Å}) = 5.08$ barn [A1]) for two different geometries: a flat plate and an annular sample. The intensity in the detectors is very sensitive to the thickness of the sample as well as its geometry. If we assume these two geometries for the same amount of scattering (5%, 10%, and 20% scatterers respectively as calculated via (A1) and (A5)) and assume that the samples are completely illuminated by the incident beam then we obtain the results displayed in figure A1. The corrected intensity is obtained using $I_{corr}(2\theta,E) = I_{obs}(2\theta,E)/A_{ssc}$ where $I_{obs}(2\theta,E)$ is the observed intensity. It is quite clear that there is a much stronger angle dependence for the correction factor of the slab geometry whereas the corrections are much less for the annular cell. Furthermore, an evaluation of the correction factor is impossible near the orientation angle, 130° in the present example, for the slab geometry. Therefore it is advantageous to use an annular geometry for backscattering. Note that, because the beam goes through the sample twice on HFBS, the sample transmission due to the presence of absorption must be <u>squared</u>.
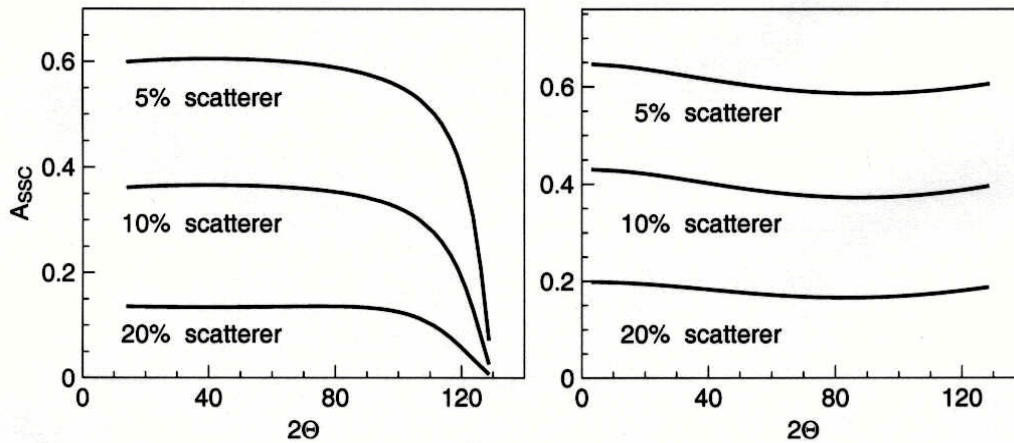

Fig.A1: Scattering angle dependence of the shelf-shielding correction factor for (a) flat plate whose normal is oriented 130 degrees with respect to incident beam direction and (b) an annular sample geometry.

When one increases the thickness of the sample for a system with a medium absorption cross-section the intensity will not significantly increase but the effects of multiple scattering will certainly be enhanced. Corrections for multiple scattering are not trivial and, for many systems in which the scattering function is not known a priori, may not be possible at all.

Figure A2 illustrates the effects that multiple scattering can have on a system, in this case viscous glycerol. This sample was measured on the IN10 backscattering spectrometer at the ILL at a temperature where the structural relaxation (viscous flow) is on the time scale of the instrument (0.1–1 ns). There is a clear broadening of the lineshape with increasing Q (FWHM ~ Q^2) due to the dynamics of the system. However at $Q = 0.19$ Å^{-1} structural relaxation cannot be resolved because it is too slow at this small Q. The effective broadening in the wings is entirely due to multiple scattering.
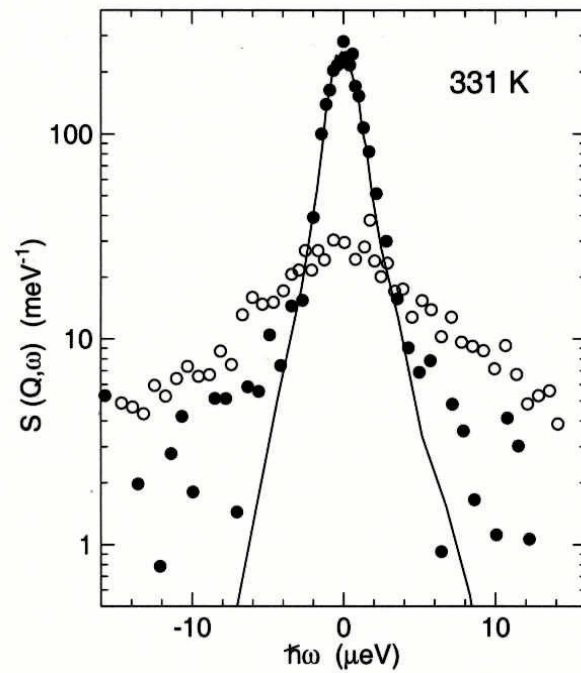

Fig.A2: Scattering intensity of viscous glycerol taken on the IN10 backscattering instrument illustrating the effects of multiple scattering on S(Q,ω). Solid line represents the instrumental resolution, open symbols are data taken at Q=1.4Å^{-1}, and the closed symbols are data taken at Q=0.19Å^{-1} [A2].

References

[A1]. V.F.Sears, Neutron News **3**, 26 (1992)

[A2]. J. Wuttke et al., Phys. Rev. E **54**, 5364 (1996)

Appendix B

Instrument Characteristics for the High Flux Backscattering Spectrometer

(http://www.ncnr.nist.gov/instruments/hfbs)

Si (111) analyzers covering 20% of 4π steradians

Si (111) monochromator 52 cm wide $\times$ 28 cm tall

$\lambda = 6.27$ Å

$E_f = 2.08$ meV

$v_n = 630$ m/s

16 ^{3}He detectors covering $14^o < 2\theta < 121^o$

Dynamic range:

-36 μeV $< \Delta E < 36$ μeV

0.25 Å^{-1} $< Q_{EL} < 1.75$ Å^{-1}

$\tau \approx 0.05 - 10$ ns

Instrumental resolution:

$\delta E < 1$ μeV (FWHM)

$\delta Q = 0.1$ Å^{-1} - 0.2 Å^{-1}

Flux at sample:

$\Phi \approx 1.4 \times 10^5$ n/cm^2/s

Beam size at sample:

2.8 cm $\times$ 2.8 cm

Signal to noise:

400:1 for vanadium foil (10% scatterer)

Sample environment:

Furnace (300 K – 1700 K)

Closed cycle refrigerator (5 K – 325 K)

Closed cycle refrigerator (50 K – 600 K)
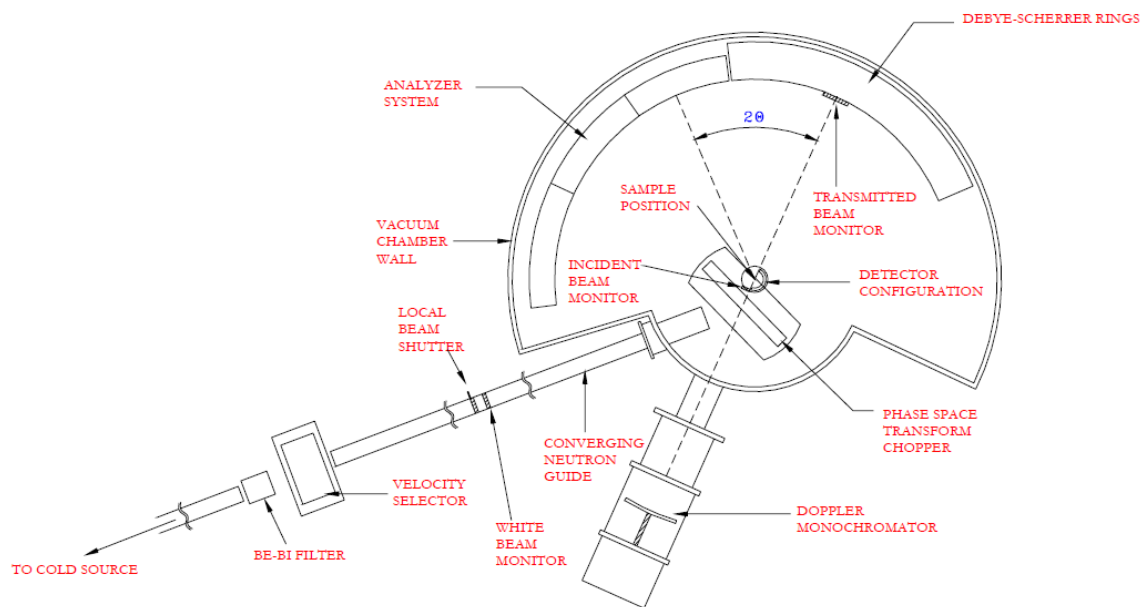
Orange cryostat (1.5 K – 300 K)

Fig.B1: Schematic of High Flux Backscattering instrument.

Appendix C

Instrumental Resolution

In an experiment with an ideal instrument we could measure the sample's scattering response directly. However real neutron spectrometers (and all measurement apparatus in general) have a finite resolution which tends to distort the measured distribution [C1]. The origin of the resolution distortion is due to many instrument-specific factors which lead to an accumulation of (hopefully small!) uncertainties. These uncertainties have the general effect of *blurring* the overall response. The effects of instrumental resolution often can be quantified in the *instrumental resolution function*. Mathematically, the resolution function and the intrinsic scattering function are convolved to yield the measured response. We present here an example of a convolution of two functions and the effects of the resolution width.

In this example we assume that the resolution function, R(E), is a normalized Gaussian centered at zero,

$$R(E) = \frac{1}{\sqrt{2\pi\sigma^2}} \exp\left(-\frac{1}{2}\left(\frac{E}{\sigma}\right)^2\right) \tag{C1}$$

and the intrinsic scattering function, S(E), is a triangle function centered at zero with a base, Δ, one unit wide ($\Delta=1$) and unit height,

$$S(E) = \frac{2}{\Delta}\left[\left(E+\frac{\Delta}{2}\right)\theta\left(E+\frac{\Delta}{2}\right) - 2E\theta(E) + \left(E-\frac{\Delta}{2}\right)\theta\left(E-\frac{\Delta}{2}\right)\right] \tag{C2}$$

where $\theta(E)$ is the unit step function.

The measured response, I(E), is given by the convolution integral,

$$I(E)=R(E)\otimes S(E)$$
$$=\int d\tilde{E}\ R(E-\tilde{E})S(\tilde{E}) \tag{C3}$$

where $\otimes$ denotes the convolution operation and the integral is over all values of $\tilde{E}$. When the Gaussian width parameter σ is small, the Gaussian approaches a delta function, and the result of the convolution looks very similar to the original triangle function. Figure C1 shows this result for a full-width at half maximum (FWHM) of 0.01. When the FWHM is larger, the resulting convolution product looks more distorted and blurred. Figure C2 shows such a case when the FWHM is 0.5.
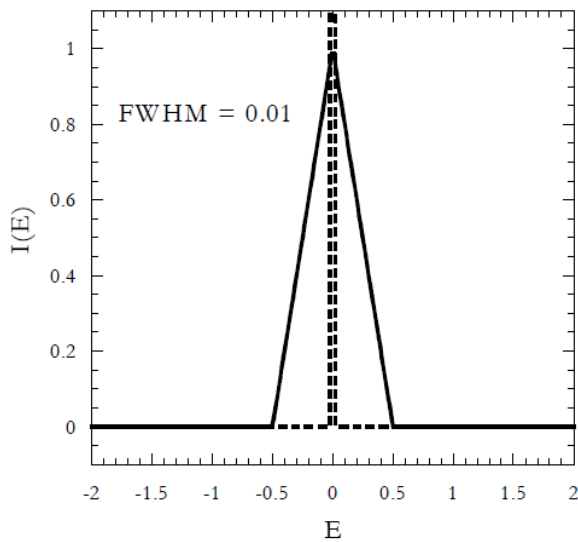
Fig.C1: Result of the convolution of the triangle function with a Gaussian of FWHM of 0.01.
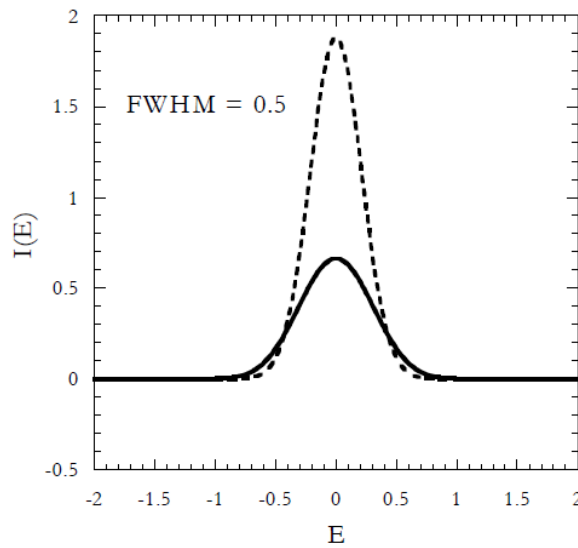

Fig. C2: Result of the convolution of the triangle function with a Gaussian of FWHM of 0.5.

Note that as R(E) becomes more narrow, the convolution product looks more like S(E). For a δ-function R(E), the convolution product is <u>exactly</u> S(E). Knowledge of the instrumental resolution function is essential for detailed lineshape analysis. Often this can be measured using an elastic scatterer.

In many cases, the instrumental resolution can be measured directly and used in the model fitting procedure via the convolution product. If we measure the scattering function from a purely elastic scatterer (ignoring the angular or Q-dependence for now) then the measured quantity is directly proportional to the resolution function. In particular, the elastic scattering function can be represented by a Dirac delta function with area A: $S_{EL}(E) = A\delta(E)$. When convolved with the resolution function, we get the measured response:

$$I_{meas}(E)=A\times\delta(E)\otimes R(E) = A\times R(E) \qquad\qquad C4$$

Note that we must normalize the resolution function so that it has unit area. This is necessary so that we can extract the integrated intensity of the intrinsic lineshape, S(E), from the fit to the model. Since the integrated intensity of the convolution product of two functions is equal to the product of the areas of the two functions then, if one of the areas is unity (as in the case of a normalized resolution function), the other must be the total area of the measured intensity.

References

[C1]. J.T.Grissom and D.R.Koehler, *Am.J.Phys* **35**, 753 (1967).